Image-Based Cell Quality Assessment: Modeling of Cell Morphology and Quality for Clinical Cell Therapy

Hiroto Sasaki, Fumiko Matsuoka, Wakana Yamamoto, Kenji Kojima, Hiroyuki Honda and Ryuji Kato

Abstract In clinical tissue engineering, both safety and effectiveness are definite requirements that should be satisfied. Conventional cell biology techniques are facing limitations in the quality assurance step of cell production for clinical therapy. Image-based cell quality assessment offers a great potential, because it is the only way to non-destructively and repeatedly assess cellular phenotypes and irregularities. To effectively assess cell quality using the multiple parameters derived from time course cell imaging, machine learning models, which have been effectively used to connect biological phenomena with biological measurements in the field of bioinformatics, are promising approaches for achieving high accuracy. Here, we present the recent results of our successful cell quality modeling and discuss its possibility and considerations on further application in clinical cell therapy.

1 Introduction

In clinical tissue engineering and cell therapy, although the cell is a "live material" with great variety and a highly sensitive nature, its production should be strictly controlled for safe and effective therapy.

If cellular irregularity is overlooked, it could cause serious side-effects such as tumorigenesis [14]. If cell yields do not fulfill the criteria on the day of the operation, the operation has to be cancelled or the cells be used with less activity.

H. Sasaki · F. Matsuoka · W. Yamamoto
K. Kojima · H. Honda · R. Kato (✉)
Department of Biotechnology, Graduate School of Engineering,
Nagoya University, Furocho, Chikusaku, Nagoya 464-8603, Japan
e-mail: kato-r@nubio.nagoya-u.ac.jp

Stud Mechanobiol Tissue Eng Biomater (2013) 10: 207–226
DOI: 10.1007/8415_2012_132

Published Online: 14 February 2012

If cell growth is unexpectedly slow during expansion culture, clinicians have to waste precious time waiting for its recovery, and cannot schedule the operation. During this process, costly consumables are wasted, and future cell behavior is most likely unpredictable. If cellular activity (e.g., differentiation rate, cellular growth, protein production, etc.) is disturbed by unresolved technical errors, the therapeutic effects of the cells will not be as expected. Hence, the many unsolved problems associated with quality assurance in clinical cell therapy should be conquered by technological achievements.

Despite the existence of such ambiguous problems in clinical cell therapy, conventional assay technologies in biology have not yet conquered any of these problems. Furthermore, conventional molecular biology assay techniques are basically incompatible with the production of cellular products, because they lack the 4 major characteristics listed below.

The first and the most fundamental criterion is non-invasiveness. Cells for clinical application should be as intact as possible, because the artificial manipulation process itself could trigger cellular abnormalities. In addition, cells derived from patients are usually limited, considering the limited source of cells and reduction in the patient's load during collection of source cells. For greater safety, fluorescent staining or gene transfer should be avoided.

The second characteristic is exhaustiveness. In clinical cell therapy, "sampling check" is a commonly used method for cell assessment. However, compared to chemical compound production, human cells exhibit huge variances; hence, partial sampling will not assure the quality of the cell population. Therefore, assessment of cells used for clinical purposes should shift to "total cell assessment" with technological advances.

The third property is synchronism. Given that cultured cells differ drastically with respect to their individual mobility, duplication, senescence, differentiation, and production activity, end-point assays are associated with high error rates. Kinetic examination is expected to detect small irregularities in cells for monitoring cellular status and optimizing cell culture conditions. High error rates together with the lack of speed limits the use of end-point assays. Most cellular contamination checks require hours, days, or weeks. This problem forces the patients to wait to be informed of problems in the implanted cells until after the operation. For practical cellular assessment, "on-time" evaluation right before the operation would strongly assist the doctors.

The fourth characteristic is correlation with future status. However accurate the on-time monitoring results of conventional assays may be, they do not quantitatively predict the future state. Therefore, in the cell production process, planning effective protocols to revise the current cell culture process for better production is extremely difficult. To enable the smooth operation of clinical cell therapy, future state prediction would facilitate the development of new clinical protocols. Because cells are not uniform and change with time, the culturing process should be optimized in an ongoing manner using effective "feedback information" with the future results in mind. Such a feedback information loop of cell quality information will improve the quality of the final cellular product, resulting in

greater therapeutic effects. Furthermore, from the clinical doctors' perspective, proper scheduling of surgery is essential for treating more patients in a given facility.

To satisfy all the above-listed criteria, "image-based cell quality assessment" offers great potential for quality assurance in cell therapy. Image-based cell quality assessment enables non-invasive, fully exhaustive, timely, and predictive evaluation of cells.

Technologies that evaluate and assess cellular activities using cell image measurement methods are being reported [3, 4, 6, 8–11, 13, 16–24, 26]. Takagi has widely reviewed especially the non-invasive cell-imaging technologies, and has introduced novel technologies. The reviews strongly indicate that cellular morphologies significantly correlate with cellular activities. These findings underscore the importance of cellular morphology monitoring in traditional cell culture methods. Many textbooks have indicated that cellular morphology is an indicator of cell quality, and therefore, it should be carefully monitored. In many facilities that offer clinical tissue engineering therapy, cells are maintained and controlled during the culture process by the experts' experienced "visual expertise." Considering the successes of image-based cell assessments and the strong requirements in clinical cell therapy, analysis of datasets of morphological features and biological phenomena are attractive for machine learning researchers. In recent years, machine learning algorithms that have been widely applied in the field of bioinformatics and systems biology (gene analysis, mRNA profile analysis, protein data analysis, etc.) have been effectively used in image-based cellular analysis studies [1, 5, 15]. However, as far as we recognize, studies using non-labeled cellular images are still limited. Furthermore, applications of machine learning algorithms to assist with cell quality assessments, especially focusing on the requirements of cell therapy, are rare.

In this book chapter, we present some of our successful modeling results that support the effectiveness of machine learning applications in clinical tissue engineering and cell therapy.

2 Strategy of Image-Based Cell Assessment Model Construction

The construction of a model for image-based cell quality assessment comprises 4 major steps: (1) Image data collection, (2) Image processing, (3) Experimental data collection, and (4) Modeling (Fig. 1).

In our studies, image data comprise phase contrast microscopic images, because they represent the type of images most frequently used by cell biologists therefore considered to contain historically-proven indicative information. For image data collection, we use BioStation CT (Nikon Corporation, Tokyo, Japan), the fully automated cell incubation and monitoring system for stable, periodical, and mass time-lapse image data. For experimental data collection, we assayed the "observed cells" using conventional cell biological techniques. From carefully selected

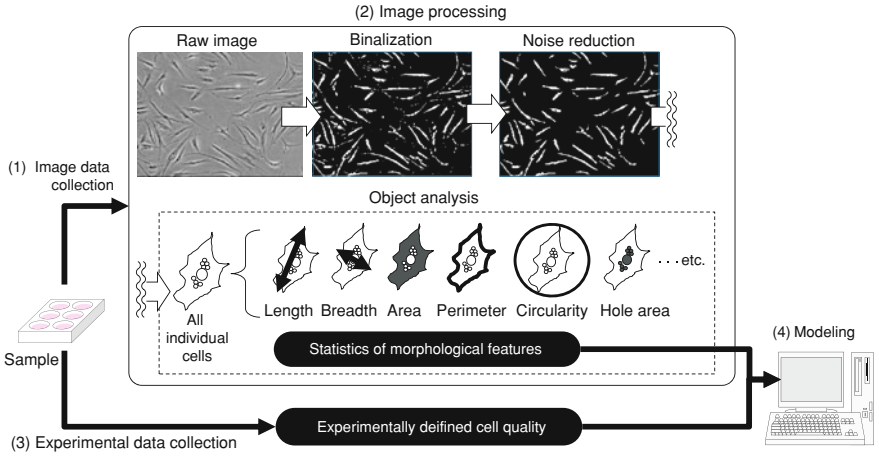

Fig. 1 Schematic illustration of image-based cell quality assessments

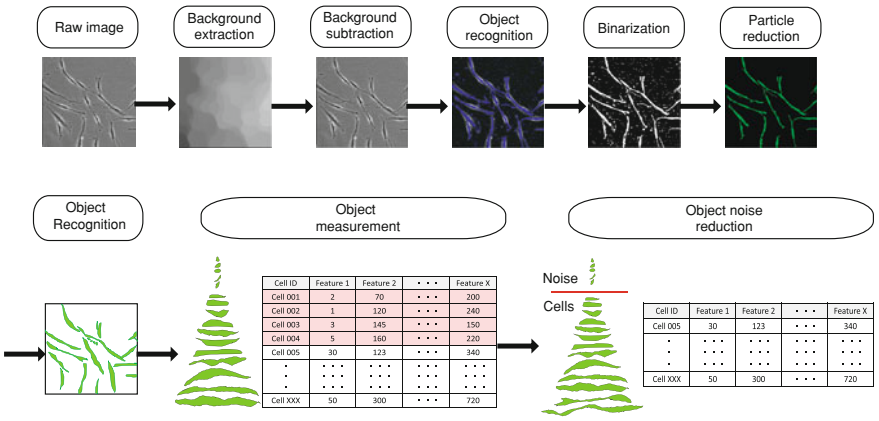

Fig. 2 Schematic illustration of image processing for assessing morphological features

assays, teacher signals can be obtained. There are cases where the culturing condition itself can be used as a teacher signal. For image processing, we customized our original image processing filters combining image analysis software and original programs in C and R languages (Fig. 2). Briefly, the raw image was processed to have the minimum error compared to manual cell counts after binarization. In this process, we applied an original combination of filters that were optimized using 26 types of human cells, including tumor cell lines and primary cells. From the objects extracted after the binarization, we measured 9–30 morphological features based on the characteristics of cells, together with multicollinearity examinations and interviews with cell culture experts. Statistical

measures from each morphological feature were tagged with the teacher signal (the target prediction value determined by the experimental data collection) and were applied as a dataset. For the modeling, we chose regression analysis models, discriminant analysis models, clustering analysis models, or neural network-based models, according to the complexity and quality of the teacher signal measurements. Further in this chapter, we present some of our successful models.

3 Regression Analysis Model for Image-Based Cell Quality Assessment

Regression is a modeling approach to understand the quantitative relationship between multiple independent variables (input features) and a dependent variable (target prediction value). During the process of constructing the regression function, users can estimate the combinational importance of various features such as "morphological features" in the case of image-based assessment. In other words, users can quantitatively understand the characteristic morphological parameter combinations that cell-culture experts unconsciously recognize and apply for their judgements.

For the target prediction value, there are various biological parameters that require prediction in clinical tissue engineering, such as cellular activity, cellular proliferation rate, cellular lineage, cellular differentiation rate, cellular production rate. Among the many candidate parameters, we chose one of the essential parameters in the cell production process, the future cell yield. The cell yield greatly affects the scheduling of operations, because most medical facilities assure the quality of cell therapy by defining the "cell number for injection." Therefore, cell culture experts are required to predict the operation date based on their expertise.

To replace such ambiguous cell production procedures, we sought to quantitatively predict the future cell yield (14 days later) of clinically obtained primary human dermal fibroblasts with multiple regression models using early cellular images (images from 1 to 3 days culture period). Fibroblasts are the cell source for skin defect and wrinkle medications already used in clinical cell therapy [2, 25]. The concept of the cell yield prediction model using cellular images is illustrated in Fig. 3.

To obtain input features from cell culture images, we collected a total of 270 phase contrast microscopic images (20 ×) of cultured primary dermal fibroblasts obtained from ten healthy volunteers (3 males, 7 females, 29–72 years old). Informed consent was obtained according to a protocol approved by the Ethics Committee of Nagoya University Hospital. Cells derived from passages 3 and 4 of the primary expansion were maintained in modified Eagle's medium (DMEM, Life technologies, Carlsbad, CA, USA) containing 10% fetal bovine serum (FBS, Life technologies) at 37°C in the presence of 5% CO_2. All images (.bmp files), manually obtained by three operators in this work, were processed using MetaMorph software (Molecular Devices, LLC., Sunnyvale, CA, USA) with

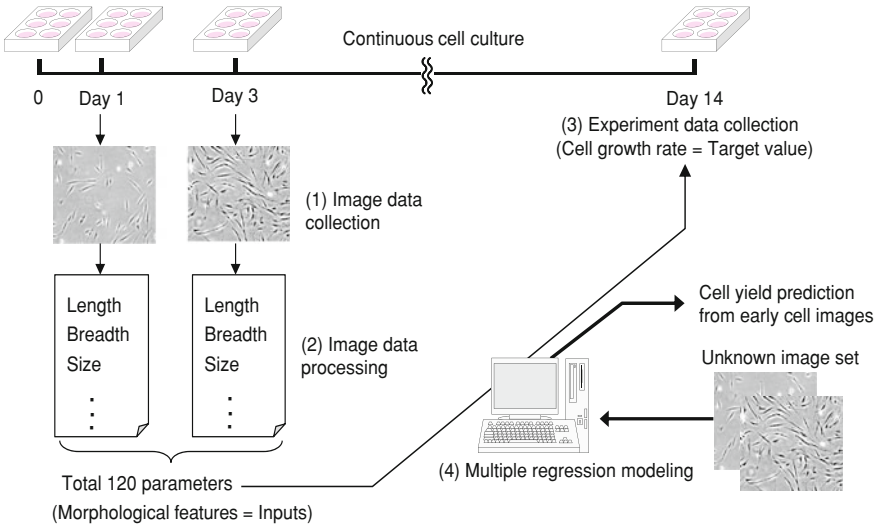

Fig. 3 Schematic illustration of the cell yield prediction model and its construction

original filter sets. Briefly, the raw images were pre-processed using open-close filters and binarized using the optimized threshold, and all objects in the image were measured with the integrated morphometry analysis process. Image data were pre-processed using the universal threshold optimized with 20 randomly picked image samples. Using integrated morphometry analysis according to the manufactuer's manual (http://mdc.custhelp.com/app/answers/list/c/110), the number of objects was measured together with 22 individual morphological features in MetaMorph, such as total area, standard area count, perimeter, width, height, orientation, length, breadth, fiber length, fiber breadth, shape factor, elliptical form factor, inner radius, outer radius, mean radius, equivalent radius, equivalent sphere surface area, equivalent sphere volume, equivalent prolate volume, equivalent oblate volume, hole area, and relative hole area. Prior to statistical analysis, morphological data from noise objects (non-cellular objects) were automatically removed using the original noise-reduction algorithm (image auto-wash method). Statistics were calculated with each measured feature in five view fields from the same well. For each feature, (a) average of day 1, (b) standard deviation of day 1, (c) average of day 3, (d) standard deviation of day 3, (e) average ratio of the day 1, and day 3 averages, (f) average ratio of the day 1 and day 3 standard deviations, were calculated as input features. From a total of 184 input features, 120 features with a CV (coefficient of variation) of <20 were used as inputs in the modeling. Input features were selected by stepwise parameter selection in the multiple regression model analysis using SPSS software (for Windows 11.5.1, IBM, Armonk, NY, USA).

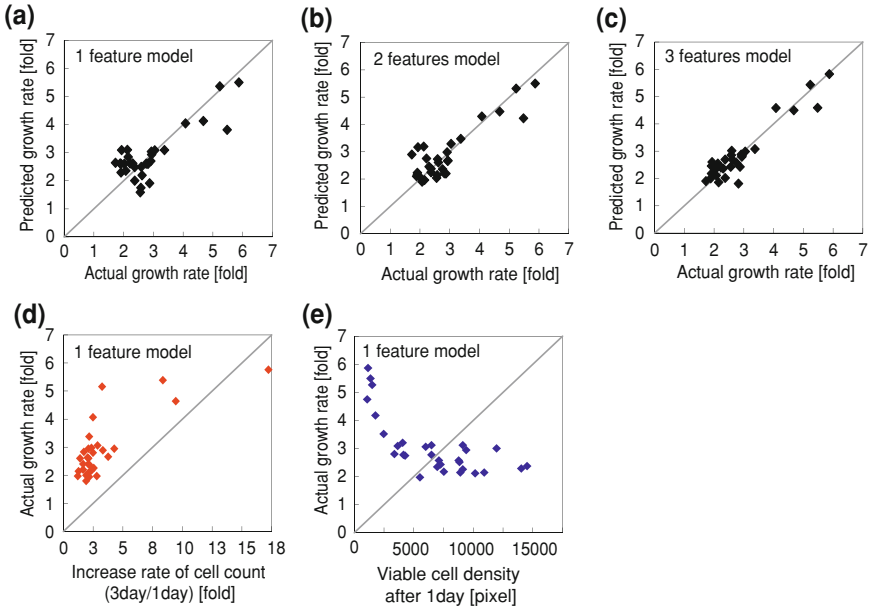

Fig. 4 Results of prediction using cell yield prediction models. **a** Prediction model using 1 feature input. **b** Prediction model using 2 feature inputs. **c** Prediction model using 3 feature inputs (the best prediction model). **d** Correlation plot of growth rate and 1 selected feature (cell density on day 1). **e** Correlation plot of growth rate and 1 selected feature (cell growth rate (day 3/day 1). Each plot represents 1 image dataset. Morphological features in models **a** **b**, and **c** were selected by a stepwise parameter selection process during model construction. The selected parameters were (P1) change rate of the standard variation of elliptical form factor (day 1–3) (P2) size of inner radius on day 3, and (P3) cell number on day 1. Morphological features in models **d** and **e** were selected on the basis of the "feeling" of a cell culture expert

To obtain the teacher signal or the target prediction value, which is based on the experimental data, three volunteers counted the partial sample of the total cell suspension from three different wells to estimate the average cell yield after 14 days of culture, and calculated the cell growth rate as the ratio of cell yield to the seeding cell number. The cell growth rate was used as the quantitative teacher signal in the modeling.

Among the 120 parameters extracted from the image data, three parameters, change rate of the standard variation of elliptical form factor (day 1–3) (P1), size of inner radius on day 3 (P2), and cell number on day 1 (P3), were found to be the best combination of cell morphology information for predicting future cell yield (average squared error = 0.14). If ±0.5 error can be accepted by the medical facility, the predict performance of this model is 87%.

The rise in prediction accuracy of models using different numbers of input features strongly indicated that multiple feature combinations provide higher prediction accuracy (Fig. 4a–c). As a comparison, it is interesting that other single parameters, intentionally selected by cell culture experts, correlated poorly with

cell yield. The correlation ratio of the model using increase rate of cell count was 0.50 (Fig. 4d), and the model using viable cell density after 1 day was 0.59 (Fig. 4e). These results strongly suggest that morphological feature selection combined with not only "morphologies" but also "changes of morphologies" is effective in image-based analysis. Since many previous image-based cell analysis works depend on "intentionally selected" morphological features, our work points out the importance of introduction of machine learning approach to construct better models for practical usage. Cell count, one of the easiest parameter that could be raised for cell yield prediction, was selected in the best prediction model. However, it should be noted that cell count was the "last parameter" selected for constructing the model, indicating that it only works in combination with morphological information. This is also clear from the above-compared prediction results in the model using a single parameter, "cell growth rate." Together with such combinational effects of parameters, another important finding using this model is that the "exact period of culture" was quantitatively pointed out. For example, cell count (nearly equal to cell growth) is important in the first 24 h, and not very informative in the latter period. Such a timing definition is extremely important for setting the image acquisition schedule, and also for defining the prediction date in the early cell culture process.

Fibroblasts change their morphology from the sharp spindle shape to the flat and polygonal shape when their growth activity decreases. The automatically determined combination of morphological parameters directly correlated with this known morphological change, indicating that the expert's feeling could be effectively modeled with this technique.

From the data, we arrived at three conclusions: (1) morphological cell information is informative for cell growth prediction, (2) objectively selected parameters are more effective in cell growth prediction than the ones selected on the basis of feeling, and (3) a combination of multiple parameters is more effective in the prediction than a single parameter. It should also be noted that such quantitative cell quality prediction can be further extended to cell differentiation rate prediction [7]. Kagami et al. [7] have shown that osteogenic differentiation status of human mesenchymal stem cells after 2 weeks of cell culture could be predicted by the morphological features priorily.

4 Discriminant Function Model for Image-Based Cell Quality Assessment

Discriminant function analysis is a statistical analysis to predict a categorical dependent variable using one or more continuous or binary independent variables. Compared to the regression analysis model, the discriminant function model satisfies clinical cell therapy requirements for assessing "binary categorical events." This is because many events in the cell production process cannot be quantitatively measured or measured data is usually categorized even if they could

be measured quantitatively. For example, bacterial contamination is the most well known risk in the cell culture process. The contamination can be measured by colony-forming assays or quantitative polymerase chain reaction (PCR) of bacterial markers. However, the quantity of contamination is meaningless in a model, because any amount of contamination should be eliminated from the process. In such cases, a decision should be made as "yes, OK to continue" or "no, discard the sample," and simple discriminant function models are effective in incorporating combinational features in the binary decision with high accuracy.

For discriminant function analysis, we designed a model to detect "human processing error", because from the aspect of establishing more safe cell production process, detection of "processing error" is essential. Practically, we attempted to model various types of human error that could be involved in the culture process and considered to affect the cellular damage rate. In various studies, we succeeded in constructing a model to detect the "error in trypsin treatment." Trypsin treatment is an essential step in subculture to digest the cellular adhesion molecule and collect cells from the culture plate, although known as a physical stress that damage cells. Some delicate cells are known to be very sensitive to trypsin concentration, and in such cases, a very low trypsin concentration is recommended. Commonly, protocol of trypsin treatment is fixed in the medical facilities' standard protocols. However, if the human error in diluting such a damageable solution can be non-destructively monitored, the model can assist the rigid protocol in the cell production process, and can reduce costly error-monitoring process of additional manual checks. The concept of the human error detection model using cellular images is illustrated in Fig. 5.

To obtain input features from cell culture images, we collected a total of 450 phase contrast microscopic images (10×) [3 wells × 5 fields × 15 time points (24–136 h, every 8 h) × 2 treatment conditions (0.25%, 0.025%)] of primary human gingival fibroblasts obtained from healthy volunteers (22 and 24 years old, female and male) and cultured in DMEM (Life technologies) containing 10% FBS (Life technologies) at 37°C in the presence of 5% CO_2 by BioStaion CT(Nikon Corporation). All images (.bmp files) were processed using MetaMorph software (Molecular Devices) and our original programs with original filter sets, as described for the regression analysis model. Using integrated morphometry analysis, the number of objects was measured together with seven individual morphological features in MetaMorph, such as total area, breadth, fiber length, fiber breadth, shape factor, elliptical form factor, and inner radius. Prior to statistical analysis, all morphological data of the noise objects (non-cellular objects) were automatically removed by the original noise-reduction algorithm (image auto-wash method). The features were averaged in 5 view fields from the same well. For each feature, average and average change ratio were calculated for and between each time point (24, 48, 72, and 96 h), and a total of 203 features were used as input features. In the modeling process, input features were selected by stepwise parameter selection in the linear discriminant analysis using SPSS software (for Windows 11.5.1).

For the target event, we intentionally designed two conditions of trypsin treatment during cell passage: 0.25% trypsin treatment (too dense = error) and 0.025% trypsin

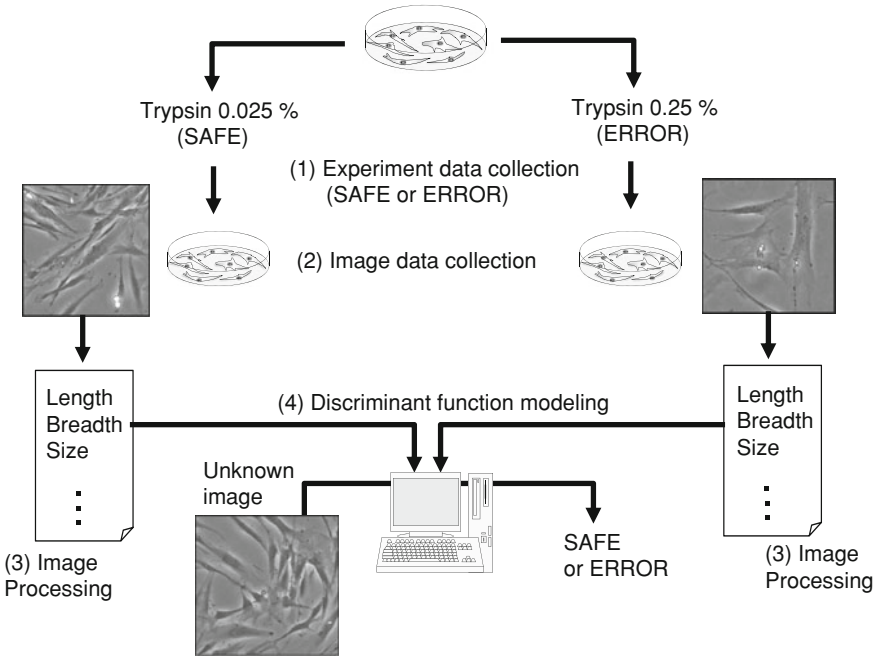

Fig. 5 Schematic illustration of the human error detection model and its construction

treatment (normal density). When cell images were collected using the former condition, the operation category was labeled as ERROR, and when cell images were from the latter condition, the operation category was labeled as SAFE.

From the 203 parameters, elliptical form factor at 24 and 48 h, breadth change between 72 h and 96 h, and fiber breadth change from 72 to 96 h were selected (Fig. 6). Damaged fibroblasts are known to lose their sharp spindle shape morphology and convert to a flat and polygonal shape; both morphological features were considered to indicate the same "morphological pattern." Interestingly, the "period of morphological change" was determined by this modeling. The "narrowness" of the first 2 days was important, but the damage from the error handling also affected the rate of morphological change during the later period (72–96 h). The prediction accuracy was 92.9%; such "operation error" is impossible to detect with conventional biological measurements.

5 Clustering Model for Image-Based Cell Quality Assessment

Clustering is a modeling approach to understand the similarity between objects by assigning them to groups. One of the features that make clustering a useful modeling method is that it enables "multi-class prediction." Biological quality,

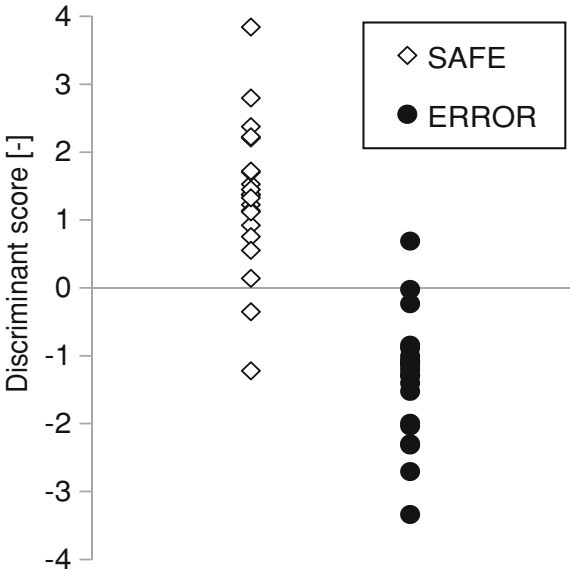

Fig. 6 Prediction results from the human error detection model. Each plot represents 1 image dataset. Morphological features in the model were selected by a stepwise parameter selection process during model construction

which relates to cells in clinical cell therapy, is often very complicated and ambiguous. Machine learning researchers should be aware that most cellular qualities are too complex to define using a single value. For example, although various biomarkers to define "stemness" of cells are measured, there exist various profiles because not all the markers are completely the same in cells. Therefore, even with the detailed profiling of biomarkers with flow cytometry analysis, cell qualities are commonly discussed as "levels" or "categories." There are many more examples of such categorical definitions of cell qualities, such as cell lineage or cell damage rate. For such cellular qualities, there is still no good single marker to define the phenomenon quantitatively.

Among such complex quality conditions of cells, "cell-type classification" is a strongly required solution in clinical cell therapy. In clinical cell therapy, a cell source is obtained from the tissues of patients. Cells are isolated from tissues by a process of primary culture, including enzyme digestion and explant culture process. Because a tissue is a complex of different cell types, there is a high possibility of incorporating "unwanted cells," which are designated as "cell contamination," in the primary cell population. For example, in the dermal defect therapy using fibroblasts, keratinocyte contamination increases the risk of dermal cyst formation. Similarly, in skin burn treatment, fibroblast contamination in keratinocytes causes a risk of skin contraction. Although such cell types are clearly known, there are still cells without good markers, such as "fibroblasts." Without a clear marker protein, fibroblasts cannot be stained or detected in the keratinocyte population. Furthermore, if clinical doctors require detection of keratinocytes among fibroblasts, staining of cells for keratinocyte-specific protein markers depletes precious patients' cell source. Therefore, "cell type classification" is an important challenge for image

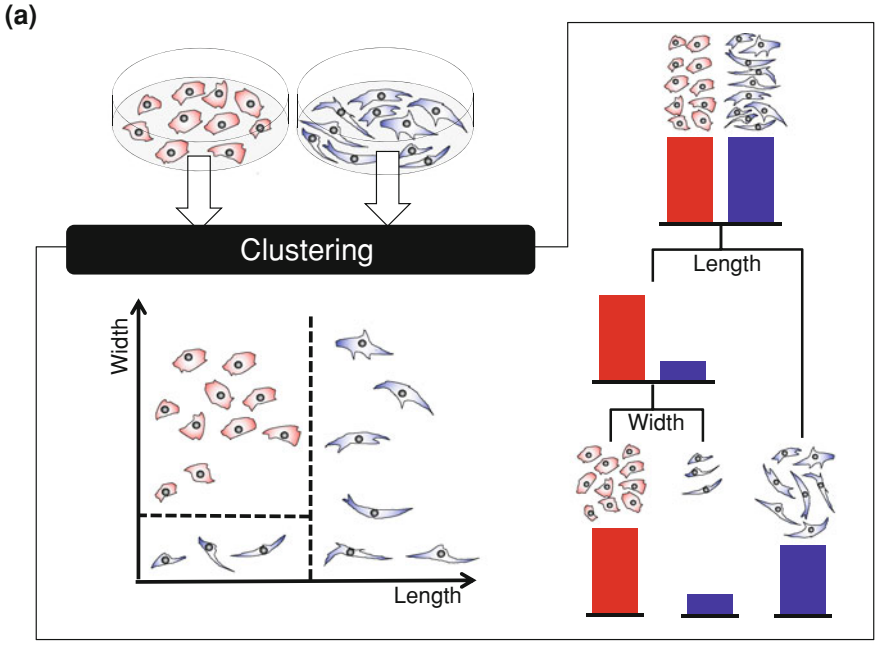
(a)
Clustering
Width
Length
Length
Width
(b)
Modeling by single cell type culture image
Test by co-culture image (contamination)
Keratinocyte
Fibroblast
Keratinocyte + Fibroblast
Learn
Test
Decision tree model
Length
Width
Length
Width
Prediction
3/5
Contamination rate
2/5

◀ **Fig. 7** Schematic illustration of the cell contamination evaluation model and its construction. **a** Schematic illustration of decision tree model for cell morphology modeling. Combination of morphological parameters (*left*) could be determined using decision tree (*right*). **b** Practical scheme for constructing cell contamination evaluation model. Model can be constructed by single cell type culture images if all cell objects could be effectively extracted from the image data. From the unknown image of co-cultured cells, fibroblasts mixed in keratinocytes in this case, the constructed model can predict the contamination rate

analysis. Considering the existence of "sub-populations" in both types of cells, a multiple-grouping method, decision tree modeling, was applied. The concept of the cell contamination evaluation model using cellular images is illustrated in Fig. 7.

To obtain input features from cell culture images, we collected a total of 270 phase contrast microscopic images (10 ×) of cultured normal human dermal fibroblasts (NHDF; KURABO, Osaka, Japan) and normal human epithelial keratinocytes (NHEK; KURABO) grown at 37°C in the presence of 5% CO_2. NHDFs were maintained in modified Eagle's medium (MEM, Life technologies) with 10% FBS, and NHEKs were maintained in EpiLife-KG2 (KURABO). For image acquisition, NHDFs were mixed with NHEK (0%/1%–30%/100%) in an NHDF contamination model of NEHKs. A total of 1912 phase contrast microscopic images (4×) were acquired from five view fields per well of a six well plate over 8 h periods for 5 days using BioStation CT (Nikon Corporation). All images (.bmp files) were processed using MetaMorph software (Molecular Devices) and our original program with original filter sets, as described in the prior section. Using integrated morphometry analysis, the number of objects was measured together with 19 individual morphological features in MetaMorph, such as total area, hole area, relative hole area, perimeter, width, height, length, breadth, fiber length, fiber breadth, shape factor, elliptical form factor, inner radius, outer radius, mean radius, equivalent radius, pixel area, area, orientation. From both cell types, totally 2,792,527 objects were measured with these morphological parameters. In the modeling process, input features were selected by recursive partitioning and regression tree (rpart) modeling using R statistics.

For the modeling of teacher signals in rpart, we carefully classified the cellular morphology types of both cells, and identified nine types of objects in the image data: (1) F_n: objects with the most typical fibroblast morphology (2) F_s: objects with small fibroblast morphology in the process of expansion (3) F_o: objects that represent a fusion of several overlapping fibroblasts (4) K_n: objects with the most typical keratinocyte morphology (5) K_s: objects with small keratinocyte morphology in the process of expansion (6) K_o: objects with holes after binarization, indicating the halo in the middle of cell (commonly caused by hill-top structure of cells) (7) K_c: objects with a "C" shape, indicating that the halo is relatively large in cell area (8) n_s; tiny non-cellular objects (9) n_l: long, but tiny non-cellular objects (Fig. 8). Groups 8 and 9 represented the common noise found in both cell types. From the modeling, we chose 100 objects from the total cells which fit to each cluster from 100% fibroblast and 100% keratinocyte images, constructed a decision tree model by tenfold cross validation, and examined the accuracy of the

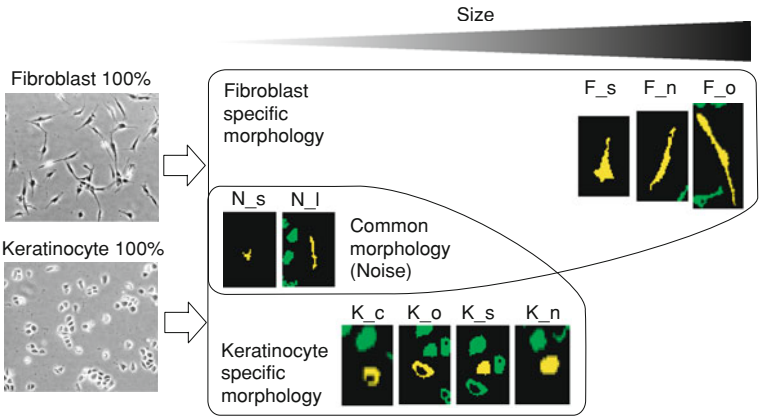

Fig. 8 Object grouping for effective decision tree construction

model for predicting the percentage of contamination of fibroblasts in keratinocytes by using only the analysis of objects from the mixed culture images.

From the clustering, nine groups of morphologically different objects found in the two cell types could be assigned to 9-clusters with high accuracy (Fig. 9). And surprisingly, although the nine-cluster model was originally constructed from the objects in 100% single cell-type images, this model succeeded in predicting cellular objects in images of co-culture (13 samples with different mixed percentages ranging from 1 to 30% fibroblast contamination in keratinocytes) with an accuracy of 93% (±5%). This prediction performance of non-labeling image cytometry is extremely high, and it should be noted that this cytometry was performed with non-stained cellular images.

The process of the decision tree modeling, i.e., the clustering with teacher signals, should provide important insights into the problem of cell classification. For cell classification, one should realize that cells are swinging between two phases of different morphologies. One is the characteristic morphology of the cell type, and the other is the round and small morphology, which is identical between all the cell types. This round and small morphology may indicate "cells before division" or "cells beginning to apoptose" or "cells in migration." With this common morphology, the classification of "individual cells" is extremely difficult. Because with the case of cells, a certain common population of objects will share exact same morphologies, and become the noise in the modeling process. The existence of such a population was very clear when we first attempted to classify the two cell types by using discrimination analysis (Fig. 10). Figure 10 shows that there is an "indiscriminative" population within each cell type. We found that such an "overlapping" population can be reduced by defining the "true-negative noise objects common to both cell types," which is represented by groups 8 and 9 in the above-mentioned criteria (Fig. 9). However, such noise reduction alone could not completely improve the prediction accuracy, because of the presence of

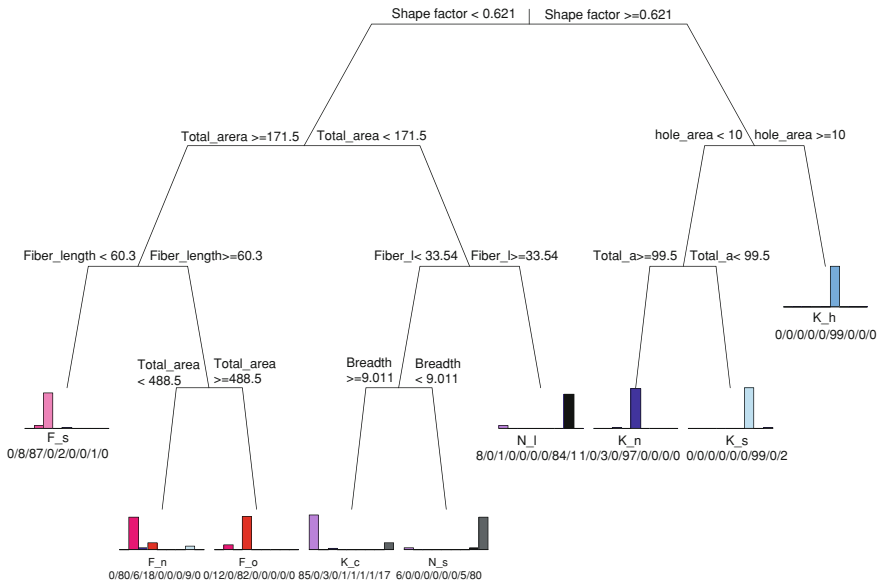

Fig. 9 Structure of the cell contamination evaluation model. The selected parameters are described in each node. Under the terminus of branches, *bars* indicate the percentage of all cell objects in the terminal node. The *numbers separated by slashes* indicates the object numbers clustered at the end branch

another "sub-population of objects" which has similar morphology and disrupts the classification accuracy. Such sub-populations are individually assigned in the decision tree model; therefore, it provided the highest accuracy in classifying the two cell types at the single cell level.

6 Discussion

Although some reports have described a connection between "morphology" and "cell quality," few reports focus on the practical tasks and problems associated with clinical cell therapy or demonstrate the effectiveness of various machine learning model approaches. Therefore, in this chapter, we have reviewed some of our successful studies on image-based bioinformatics modeling in clinical cell therapy.

Image-based cell assessment is gaining popularity along with the advances in "imaging equipment" and "high content analysis software." Indeed, machine learning approaches are important for the analysis of "multi-variant data measurements" together with "biological complex phenomena." Bioinformatics, widely applied in the research fields of DNA microarray, SNP typing, and proteome data mining, has been the leading application in the field of machine learning algorithms. Image-based data analysis may be the next frontier.

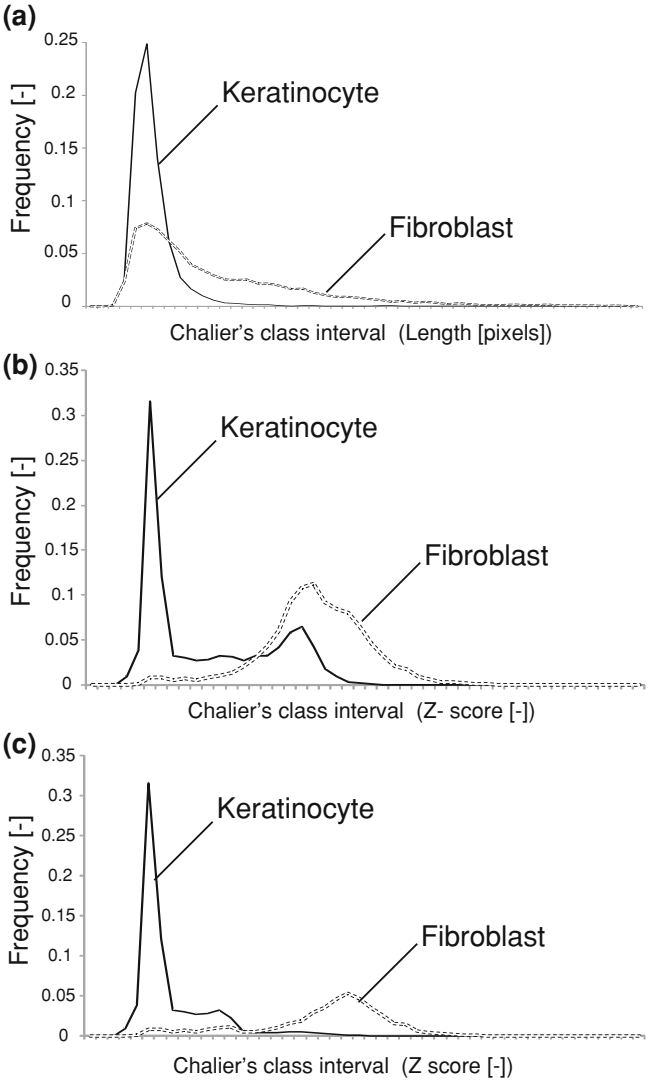

Fig. 10 Parameter distribution comparing keratinocytes and fibroblasts. **a** Distribution of length between two types of cells. There is huge overlapping area in one parameter distribution. **b** Distribution of Z-score from the discriminant analysis using 19 morphological features between two types of cells. There is still overlapping area even after the discriminant modeling. **c** Distribution of Z-score from the discriminant analysis using 19 morphological features using "noise reduced data". Noise objects were excluded from the discriminant analysis by eliminating the group N_s and N_l objects from the data. Such noise data **c** reduction greatly reduces overlapping area from cell distributions

However, many important points have been neglected in the recent image-based biological analyses. Although machine learning approaches offer strong prediction performances, analysts should be aware of the problems arising from the combination of "nature of image data" and "nature of cells."

First, cellular image data has a much higher bias compared to mRNA and protein data. This is because mRNA and proteins are total molecules summed within all the cells in one vessel, whereas image data biases depend on where and by whom the cells are observed. Typically, cells grow locally in culture dishes, and migrate toward empty spaces. Thus, if cells are not uniformly seeded, the cell number and migration rates differ greatly between images. Furthermore, analysts should be aware that most cellular images from cell biologists are taken from the researchers' favorite "view field" with favorite "focus and lighting." Therefore, if images are not acquired randomly or scheduled by automated machinery, random selection of images from the "researcher's image library" already has a huge bias.

Second, due to the nature of cells, cellular images always contain a certain percentage of "common features." This is because every cell type exhibits the same round and small morphology when the cells are "dead," "proliferating," or "rapidly migrating." In addition, cell-derived debris increases on the surface of the culture plate during the culture process. Such a "common sub-population," which contributes to fatal noise in machine learning algorithms, drastically lowers model accuracy. Therefore, the objects in cellular images have to be effectively filtered or classified by detailed observation and statistical analysis of the cell populations before model construction. We also have to consider the fact that primary cells sometimes contain "different cell types," although they are usually overlooked.

Third, the cell variation is huge between cell lines, cell passages, and cell origins. Therefore, the variation arising from the source of cellular images is also extremely important. In our experience, such variation is extremely large; therefore, the quantity of images should be large enough to provide enough cell numbers to minimize the standard deviation. Such quantity and variation in cellular images are commonly neglected, mostly because of the cost and labor involved in the experiment. For effective machine learning, sufficient data for cross-validation is required; therefore, the experimental design for image acquisition is extremely important.

Fourth, cellular image processing is commonly completely dependent on the researcher's feeling. In most cases, binarization is processed with "a threshold." However, this threshold is commonly decided by some value "considered OK by the researcher after evaluating fewer than 20 images." Such a threshold is rarely "thoroughly scanned," because such a function is lacking in most cellular image analysis software. Therefore, most cellular images are processed individually and differently with a "feeling-based threshold," or processed by a single threshold that is "roughly decided." Therefore, a high bias is inherent in image processing when image data are processed into numerical data.

To reduce these four major biases, we applied original solutions before analysis. (i) Image bias: we used an original seeding device for equal cell seeding, and acquired more than 400 images per condition, including different view fields, wells, and time-

points. We also used a fully auto-scheduled and auto-focusing image acquisition system, BioStation CT (Nikon corporation) to minimize the image acquisition bias. (ii) Population bias: we have shown that population bias can be classified using decision tree models, too. We also remove the "common population" before analysis by using our original noise-reduction algorithm. (iii) Cell and culture bias: we routinely used three or more lots or passages of cells in every experiment. We also set image acquisition periods of less than 8 h to obtain more information during the average doubling time. (iv) Processing bias: we optimized the universal threshold by examining the threshold ranges of randomly picked images from 5 to 10 cell lines at different time-points for the best threshold that resulted in minimum error in the cell count. We also strongly recommend using pattern matching algorithms to recognize objects in the image, such as the software "CL-Quant (Nikon Corporation).

To assist clinical cell therapy with such machine learning models combined with image analysis, "what to predict" should be carefully researched. There are strong expectations and requirements in clinical cell therapy toward non-invasive cell quality assessments. A large number of "qualities" and "events" are expected to be predicted in the clinical setting. However, to build a prediction model, the teacher signal should be carefully selected and defined. For example, beta galactosidase activity is a biological marker of cellular senescence [12]. However, the efficiency of beta galactosidase detection in a single stained image is actually very low. It may correlate with senescence when the data are averaged in "1 well," but not in "images that do not cover all the wells." In such cases, differences in detection power exist between biological assays and image detection. Without knowing the detection power of the target event, inconsiderate modeling and data acquisition will result in no harvest. Moreover, there are some cases where a "1 marker measurement" is not sufficient for definition. For example, in the case of defining stemness of cells, the single marker staining result would not produce the expected stemness prediction model.

Additionally, the "acceptable accruracy" of model should be also carefully discussed by the users of these machine-learning models for cell quality evaluations. The accuracy should also be carefully checked with the aspect of consistency and reproducibility. In many cases, the non-labeling and real-time estimation of cell quality are difficult to compare its performance with conventional methods, because the image-based cell quality assessment has uncomparable advantage features. However, such comparison difficulty never means that conventional assay can be eliminated. The acceptable accuracy of models should be defined by each medical facility with their specific verification data, and should be used only to reduce the excessiveness and unstableness in the conventional cell production process.

7 Conclusion

Machine learning modeling algorithms have great potential in image-based cell quality assessments. Based on the selection of appropriate models with sufficient quantities of images for predicting target events, our results suggest a potential of

non-labeled and real-time assessment of cellular quality strongly required in the present industrialization era of tissue engineering and regenerative medicine. Our results, most of them are newly presented in this chapter, indicate that quantitative prediction, categorical prediction, and multi-categorical classification can be achieved with high accuracy.

Like the other machine learning models in different research fields, robustness should be repeatedly examined to build universally effective cell quality prediction models. We are conducting further investigations to determine the extent of cellular variations to build a practically useful model.

We strongly expect that the feedback loop of advances and improvements in biology and computational technology will advance this field of cell assessment with bioinformatics machine learning models.

Acknowledgments We are grateful to the New Energy and Industrial Technology Development Organization (NEDO) for the Grant for Industrial Technology Research (Financial Support to Young Researchers, 09C46036a) for the support. We also thank to the Nikon Corporation for their research collaboration and financial support. We also thank Mai Okada and Yurika Nonogaki for supporting the experiments and data storage. Finally we greatly thank Yoshihide Nagura, Kazuhiro Mukaiyama, and Asuka Miwa for establishing basal techniques for our image analysis procedure.

References

1. Carpenter, A.E., Jones, T.R., Lamprecht, M.R., Clarke, C., Kang, I.H., Friman, O., Guertin, D.A., Chang, J.H., Lindquist, R.A., Moffat, J., Golland, P., Sabatini, D.M.: CellProfiler: image analysis software for identifying and quantifying cell phenotypes. Genome Biol. **7**, R100 (2006)
2. Ebisawa, K., Kato, R., Okada, M., Sugimura, T., Latif, M.A., Hori, Y., Narita, Y., Ueda, M., Honda, H., Kagami, H.: Gingival and dermal fibroblasts: their similarities and differences revealed from gene expression. J. Biosci. Bioeng. **111**, 255–258 (2011)
3. Galon, J., Costes, A., Sanchez-Cabo, F., Kirilovsky, A., Mlecnik, B., Lagorce-Pages, C., Tosolini, M., Camus, M., Berger, A., Wind, P., Zinzindohoue, F., Bruneval, P., Cugnenc, P.H., Trajanoski, Z., Fridman, W.H., Pages, F.: Type, density, and location of immune cells within human colorectal tumors predict clinical outcome. **313**, 1960–1964 (2006)
4. Harder, N., Mora-Bermudez, F., Godinez, W.J., Wunsche, A., Eils, R., Ellenberg, J., Rohr, K.: Automatic analysis of dividing cells in live cell movies to detect mitotic delays and correlate phenotypes in time. Genome Res. **19**, 2113–2124 (2009)
5. Held, M., Schmitz, M.H., Fischer, B., Walter, T., Neumann, B., Olma, M.H., Peter, M., Ellenberg, J., Gerlich, D.W.: CellCognition: time-resolved phenotype annotation in high-throughput live cell imaging. Nat. Methods **7**, 747–754 (2010)
6. Jones, T.R., Carpenter, A.E., Lamprecht, M.R., Moffat, J., Silver, S.J., Grenier, J.K., Castoreno, A.B., Eggert, U.S., Root, D.E., Golland, P., Sabatini, D.M.: Scoring diverse cellular morphologies in image-based screens with iterative feedback and machine learning. Proc. Natl. Acad. Sci. U S A. **106**, 1826–1831 (2009)
7. Kagami, H., Agata, H., Kato, R., Matsuoka, F., Tojo, A.: Fundamental technological developments Required for increased availability of tissue engineering. InTech (2010)
8. Kamentsky, L., Jones, T.R., Fraser, A., Bray, M.A., Logan, D.J., Madden, K.L., Ljosa, V., Rueden, C., Eliceiri, K.W., Carpenter, A.E.: Improved structure, function and compatibility

for CellProfiler: modular high-throughput image analysis software. Bioinformatics **15**, 1179–1180 (2011)
9. Kino-oka, M., Agatahama, Y., Haga, Y., Inoie, M., Taya, M.: Long-term subculture of human keratinocytes under an anoxic condition. J. Biosci. Bioeng. **100**, 119–122 (2005)
10. Kirillov, V., Stebenyaeva, E., Paplevka, A., Demidchik, E.: A rapid method for diagnosing regional metastases of papillary thyroid cancer with morphometry. Microsc. Res. Tech. **69**, 721–728 (2006)
11. Kittler, R., Pelletier, L., Heninger, A.K., Slabicki, M., Theis, M., Miroslaw, L., Poser, I., Lawo, S., Grabner, H., Kozak, K., Wagner, J., Surendranath, V., Richter, C., Bowen, W., Jackson, A.L., Habermann, B., Hyman, A.A., Buchholz, F.: Genome-scale RNAi profiling of cell division in human tissue culture cells. Nat. Cell. Biol. **9**, 1401–1412 (2007)
12. Kurz, D.J., Decary, S., Hong, Y., Erusalimsky, J.D.: Senescence-associated (beta)-galactosidase reflects an increase in lysosomal mass during replicative ageing of human endothelial cells. J. Cell Sci. **113** (Pt 20), 3613–3622 (2000)
13. Logan. D.J., Carpenter. A.E.: Screening cellular feature measurements for image-based assay development. J. Biomol. Screen. **15**, 840–846 (2010)
14. Maekawa, M., Yamanaka, S.: Glis1, unique pro-reprogramming factor, may facilitate clinical applications of iPSC technology. Nature **474**, 225–229 (2011)
15. Misselwitz, B., Strittmatter, G., Periaswamy, B., Schlumberger, M.C., Rout, S., Horvath, P., Kozak, K., Hardt, W.D.: Enhanced CellClassifier: a multi-class classification tool for microscopy images. BMC Bioinformatics. **11**, 30 (2010)
16. Nafe, R., Franz, K., Schlote, W., Schneider, B.: Morphology of tumor cell nuclei is significantly related with survival time of patients with glioblastomas. Clin. Cancer Res. **11**, 2141–2148 (2005)
17. Narkilahti, S., Rajala, K., Pihlajamaki, H., Suuronen, R., Hovatta, O., Skottman, H.: Monitoring and analysis of dynamic growth of human embryonic stem cells: comparison of automated instrumentation and conventional culturing methods. Biomed. Eng. Online **6**, 11 (2007)
18. Neumann, B., Held, M., Liebel, U., Erfle, H., Rogers, P., Pepperkok, R., Ellenberg, J.: High-throughput RNAi screening by time-lapse imaging of live human cells. Nat. Methods **3**, 385–390 (2006)
19. Sekiya, I., Larson, B.L., Smith, J.R., Pochampally, R., Cui, J.G., Prockop, D.J.: Expansion of human adult stem cells from bone marrow stroma: conditions that maximize the yields of early progenitors and evaluate their quality. Stem Cells **20**, 530–541 (2002)
20. Simpson, K.J., Selfors, L.M., Bui, J., Reynolds, A., Leake, D., Khvorova, A., Brugge, J.S.: Identification of genes that regulate epithelial cell migration using an siRNA screening approach. Nat. Cell Biol. **10**, 1027–1038 (2008)
21. Takagi, M.: Noninvasive quality estimation of adherent mammalian cells for transplantation. Biotech. Bioproc. Eng. **15**, 54–60 (2010)
22. Tokumitsu, A., Wakitani, S., Takagi, M.: Noninvasive discrimination of human normal cells and malignant tumor cells by phase-shifting laser microscopy. J. Biosci. Bioeng. **109**, 499–503 (2010)
23. Treiser, M.D., Yang, E.H., Gordonov, S., Cohen, D.M., Androulakis, I.P., Kohn, J., Chen, C.S., Moghe, P.V.: Cytoskeleton-based forecasting of stem cell lineage fates. Proc. Natl. Acad. Sci. U S A **107**, 610–615 (2010)
24. Umegaki, R., Murai, K., Kino-Oka, M., Taya, M.: Correlation of cellular life span with growth parameters observed in successive cultures of human keratinocytes. J. Biosci. Bioeng. **94**, 231–236 (2002)
25. Watson, D., Keller, G.S., Lacombe, V., Fodor, P.B., Rawnsley, J., Lask, G.P.: Autologous fibroblasts for treatment of facial rhytids and dermal depressions. A pilot study. Arch. Facial Plast. Surg. **1**, 165–170 (1999)
26. Zhou, X., Cao, X., Perlman, Z., Wong, S.T.: A computerized cellular imaging system for high content analysis in Monastrol suppressor screens. J. Biomed. Inform. **39**, 115–125 (2006)